

Spectroscopic ellipsometry investigation on the excimer laser annealed indium thin oxide sol–gel films



Miru Noh ^a, Ilwan Seo ^a, Junghyun Park ^a, J.-S. Chung ^a, Y.S. Lee ^{a,*}, Hyuk Jin Kim ^b, Young Jun Chang ^c, J.-H. Park ^d, Min Gyu Kang ^e, Chong Yun Kang ^{f,g}

^a Department of Physics, Soongsil University, Seoul 156-743, Republic of Korea

^b Department of Energy & Environmental System Engineering, University of Seoul, Seoul 130-743, Republic of Korea

^c Department of Physics, University of Seoul, Seoul 130-743, Republic of Korea

^d IT Convergence and Components and Material Research Laboratory, Electronics and Telecommunications Research Institute, Daejeon 305-700, Republic of Korea

^e Department of Mechanical Engineering, Virginia Tech, Blacksburg, VA 24061, United States

^f Center for Electronic Materials, Korea Institute of Science and Technology, 5 Hwarang-ro 14-gil, Seongbuk-gu, Seoul 136-791, Republic of Korea

^g KU-KIST Graduate School of Converging Science and Technology, Korea University, 145 Anam-ro, Seongbuk-gu, Seoul 136-701, Republic of Korea

ARTICLE INFO

Article history:

Received 30 March 2015

Received in revised form

5 August 2015

Accepted 2 November 2015

Available online 10 November 2015

Keywords:

Indium tin oxide

Excimer laser annealing

Spectroscopic ellipsometry

Sol–gel

ABSTRACT

We report on the effect of the excimer laser annealing on the electronic properties of indium tin oxide (ITO) sol–gel films by using spectroscopic ellipsometric technique. We found that the excimer laser annealing effectively induces the crystallization as well as condensation of the sol–gel film. As the laser power increased, the carrier concentration and the relaxation time of photo-annealed films increased, with the bandgap shifting to higher energies. Simultaneously, the extinction coefficient values in the visible region were reduced significantly. We suggest that the excimer laser annealing should be a promising method for low temperature preparation of the ITO film on heat-sensitive substrates via the sol–gel process.

© 2015 Elsevier B.V. All rights reserved.

1. Introduction

Transparent conducting oxides (TCO) have attracted much attention due to their wide range of applications to optoelectronic devices as transparent electrodes [1–3]. A chief characteristic of TCO is the combination of high transparency in the visible region and low electric resistance. Indium tin oxide (ITO) is one of the most utilized TCO materials in modern technology. The resistivity (ρ_{DC}) of ITO could be as low as $10^{-3} \Omega\text{cm}$, and its extinct coefficient (k) in the visible region could be lower than 0.001, with wide optical bandgap (E_g) as high as 3.8 eV [4]. Fairly low resistivity results from the high carrier concentration ($n \sim 10^{21}/\text{cm}^3$) generated by the oxygen vacancy [5] as well as the substitute of Sn^{4+} for In^{3+} . The optimal Sn doping concentration has been known to be about 10%.

To extend the application of ITO to low-cost printable electronics on the plastic substrate, the solution process-ability such as

the sol–gel process [6,7] and the similar solution combustion method [8] is essential. The formation of the ITO crystalline phase in the sol–gel process requires an annealing step at relatively high temperature, $\sim 400^\circ\text{C}$. This constraint is incompatible for some heat sensitive substrates, such as polymers, with strong demand of low temperature ($\sim 200^\circ\text{C}$) preparation. As an alternative to the thermal annealing, it is pertinent to employ the photo-assisted annealing method. Indeed, the laser annealing technique has been used for enhancing the electric property of sputter-deposited ITO films [9–11]. Also, by using the deep ultraviolet photochemical method, Kim et al., succeeded in fabricating several TCO sol–gel films whose qualities were comparable to those of the high temperature thermally annealed films [7].

In this paper, we report on the significant change in the electronic properties of ITO sol–gel films by the excimer laser annealing (ELA) process. Since the ELA method is already used for rapid annealing process of poly-silicon for fabricating large area devices, such as liquid crystal displays [12] and organic light emitting diode displays [13] it is already proven that the ELA method is economically viable for the large area and possibly flexible device

* Corresponding author.

E-mail address: yilee@ssu.ac.kr (Y.S. Lee).

fabrication. This is due to compensation of the expensive laser cost by fast scanning laser pulses over large area devices. Our spectroscopic ellipsometric study clearly shows that the carrier concentration and the relaxation time of photo-annealed films were increased. At the same time, the optical bandgap was shifted to higher energies, with the absorption in the visible region suppressed significantly. We suggest that the ELA process could be a promising method for low temperature preparation of the ITO sol–gel films deposited on plastic substrates.

2. Experiment

The ITO films were fabricated in the sol–gel method [14,15]. The metal precursors of ITO, $\text{In}(\text{NO}_3)_3 \cdot x\text{H}_2\text{O}$ and SnCl_2 , were dissolved in 2-methoxyethanol (2-ME) at 0.3 M. The mixing ratio of In and Sn solutions was 9:1, which has been known as the optimal ratio for a transparent conducting behavior. With the SiO_2 (300 nm) covered Si substrates, we performed the spin-coating at a speed of 3000 rpm for 30 s. After the spin-coating, all samples were pre-annealed at 150 °C for 30 min on a hotplate (as-spun film).

The 248 nm (= 5 eV) KrF ELA process was performed at 20 Hz frequency for 30 s (equal to 600 pulses) with laser energy density $J_L = 50, 100, 150, 200,$ and 240 mJ/cm^2 [16,17]. The beam passed through a beam expander to have uniformity, an attenuator to easily control the energy density, and a condensing lens to focus beam. In particular, in order to obtain nearly uniform energy distribution, we used a square array of diffractive microlenses to convert the Gaussian beam profile into a “top hat” shaped beam profile [18]. Finally, the laser was evenly focused to a beam of $5 \times 5 \text{ mm}^2$. We note that in the ELA process one could anneal a given area within a second and scan the laser beam over large area. In addition, for large scale process, several lasers could be combined to expand the laser beam size. Therefore, the beam size of $5 \times 5 \text{ mm}^2$ in this study can be generally expandable for fabricating large area samples. The films were positioned on hot plate at 200 °C during the ELA process (ELA-ITO films). Since the flexible plastic substrates have maximum process temperature of 150–250 °C, we chose maximum process temperature of 200 °C. In addition, we experimentally confirmed that such thermal heating promotes the ELA process, so that the resulting films show higher electrical conductivity.

X-ray diffraction (XRD) patterns were measured with a Bruker-AXS Discover D8 system with a Cu target x-ray tube. The x-ray beam was focused to a parallel beam by a Gobel mirror to enhance the intensity for thin film measurement. For spectroscopic study on the ELA-ITO films, we performed the spectroscopic ellipsometry (SE) with variable incident light angles (60°, 65°, and 70°) in the range of 0.74 eV–5.5 eV at room temperature [19]. The SE machine was V-VASE (J. A. Wollam Co., Inc.). The measured ellipsometry angular spectra $\Psi(\omega)$ and $\Delta(\omega)$ were fitted with the three-layer model (ITO film + SiO_2 (300 nm) + Si single crystal) to obtain the complex optical constants of the ITO films, e.g., complex refractive index, $\tilde{n}(\omega) = n + ik$, and complex conductivity spectra, $\tilde{\sigma}(\omega) [\equiv \sigma_1(\omega) + i\sigma_2(\omega)]$. The fitting spectra are composed of Drude and Lorentz oscillator modes. Fig. 1 shows $\Psi(\omega)$ and $\Delta(\omega)$ measured with the 60° incident light angle for the films annealed with $J_L = 50$ and 240 mJ/cm^2 . The experimental and fitting data are clearly found to be consistent. To ensure that the obtained optical constants were correct, we independently measured normal incidence reflectivity spectra $R(\omega)$ for the spectral range 0.1–6 eV. As shown in the inset of Fig. 1(b), we found that the measured $R(\omega)$ agreed with the corresponding value calculated from the ellipsometry data, even in the lower energy region than in the SE measurement region, where optical data can be predicted from the fitting parameter. The combination of the SE and reflectivity

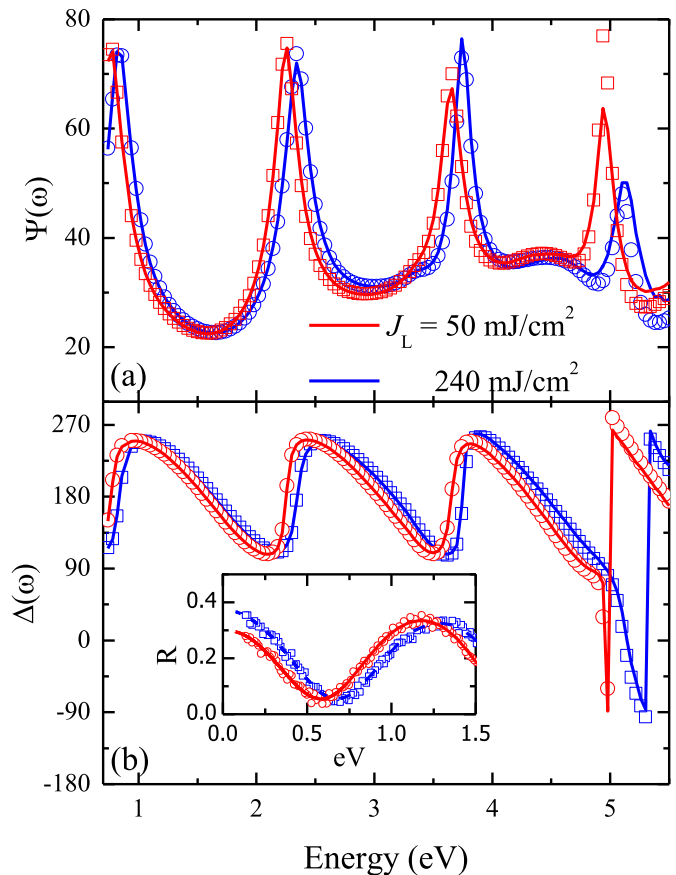


Fig. 1. Ellipsometry angular spectra, (a) $\Psi(\omega)$ and (b) $\Delta(\omega)$ for the ITO films annealed in the ELA process with $J_L = 50$ and 240 mJ/cm^2 . The fitting spectra are overlaid, denoted by the open symbols. Inset: Reflectivity spectra $\Delta(\omega)$ for the ITO films annealed in the ELA process with $J_L = 50$ (red) and 240 mJ/cm^2 (blue). The solid lines represent the measured spectra, and the open symbols represent the fitting spectra calculated from the ellipsometry results. (For interpretation of the references to colour in this figure legend, the reader is referred to the web version of this article.)

measurements provided a complete determination of the optical constants of our ITO films in the photon energy region from 0.1 eV to 6 eV.

3. Results and discussion

3.1. Structural analysis on the ELA ITO films

Fig. 2 shows XRD 2θ scan results at 3° grazing incidence for the ELA-ITO films at $J_L = 50, 100, 150, 200,$ and 240 mJ/cm^2 . The dominant peaks near $2\theta = 30^\circ$ and 35° were assigned as the ITO (222) and ITO (400) peaks, respectively [20]. In contrast to the case of $J_L = 50 \text{ mJ/cm}^2$, the XRD peaks developed significantly with the increasing J_L from 100 mJ/cm^2 . These results clearly indicated that the crystalline quality of the ELA-ITO films was enhanced as the laser power increased.

3.2. Electronic structure of the ELA-ITO films

Fig. 3 shows the real part of optical conductivity spectra $\sigma_1(\omega)$ of the ELA-ITO films. For comparison we included the optical spectra of as-spun ITO film. The spectra are divided into three regions as follows: low energy region where the charge carrier response is dominant (below 1 eV), transparent region (1 eV–4 eV), and high energy region where the interband transitions are observed (above

Download English Version:

<https://daneshyari.com/en/article/1785947>

Download Persian Version:

<https://daneshyari.com/article/1785947>

[Daneshyari.com](https://daneshyari.com)